

Traditional methods for the design of radial-axial hydraulic turbines with verification in CFD simulation

I Handal^{1,2}, V Tkachuk¹, A Petrov¹ and A Protopopov¹

¹Bauman Moscow State Technical University

²E-mail: handal.ignacio15@gmail.com

Annotation. In the modern world, the use of hydrodynamic power plants is one of the fundamental ways of generating electricity. The main part of such power plants is the hydraulic turbine impeller, therefore, for the developer, the main task is to design it correctly. In this work are used the traditional methods for designing radial-axis hydraulic turbines and test their operability with CAD and CFD programs. For that was created a hydro turbine model that will be installed in El Salvador. Subsequently, in the future, this hydroturbine will be optimized.

Introduction

Hydraulic turbines have been used for over a century and are based on reliable technology. However, growth and competition in the energy market requires an increase in electricity production at lower costs, which leads to the need to improve equipment for hydropower plants. Therefore, it is important to increase the efficiency of hydroelectric power plants, namely the efficiency of turbines.

The efficiency of the turbine can be increased by changing the parameters of the geometry of the turbine. Sequential tests are needed to increase turbine efficiency. Although it is possible to predict the characteristics of the turbine using model tests in the laboratory; time and budget constraints, prototype constraints contributed to the use of CFD tools for turbine optimization.

Each hydropower project requires a different turbine design. Preliminary design is based on experimental methods, traditional design procedures, and the hydrodynamic theory of machines. Preliminary model is subjected to CFD analysis to evaluate hydraulic performance. CFD analysis allows to determine undesirable flow conditions, such as flow separation, cavitation zones, which cannot be predicted in traditional design methods. This is an iterative process leading to optimal turbine performance. It should be noted that the maximum efficiency of the turbine is achieved not under design conditions, but under partial load. The efficiency of the turbine is slightly lower than the maximum efficiency at the design pressure and the estimated flow: this case is called the optimal operating condition of the turbine throughout the entire operation. It is worth noting that approximately 96% of hydraulic losses occur in the blades of the radial axial turbine. Therefore, the main design work is therefore focused on the rotor blades. Minor changes in the solid turbine model, especially in the rotor, result in optimized turbine geometry with optimized efficiency and flow dynamics. Problematic areas can be changed in order to achieve the target efficiency at the design load and design load. Issues related to the design and CFD simulation of hydrodynamic turbines are widely covered in the literature [1–16].



A radial-axial turbine is applicable for a wide range of head and flow rates and may be preferable to a rotary-blade hydraulic turbine due to its compactness; or bucket hydro turbine due to its higher efficiency at a better efficiency point. All those factors make the radial-axial turbine profitable, and it is the focus of this study. It has been selected to design a turbine expected to work under the following parameters.

Table 1. Turbine work parameters

Head pressure, m	Flow Rate, m ³ / s	Rotor rotational speed, rpm	Theoretical Efficiency, %	Specific speed, n _s
72	50.5	300	93	293

The radial-axial turbine design begins with the impeller, and then the guide vanes, fixed vanes and spiral casing are developed. On this article it has been only described the process to obtain the impeller geometry, nevertheless the rest of the elements have been calculated accordingly. After obtaining the theoretical geometry of the turbine, using the CFD software, it is necessary to compare the efficiency obtained at different opening angles of the guide vane.

Method

Hydraulic profile diagram, Bovet method [1]

Theodore Bovet (1964), based on hydraulic turbines already built, determined a number of speed factors to obtain the hydraulic profile of a new turbine.

A specific dimensionless speed is used

$$n_0 = \frac{n_{sync} \left(\frac{Q}{\pi} \right)^{1/2}}{(2gH)^{3/4}} \quad (1)$$

Where n: rad / s, Q: m³ / s, H: (m), g: (m / s²)

For radial axial turbines the specific number of revolutions is usually within the range of 0.1 < n₀ < 0.8. Figure 1 shows the variations of the profiles according to their n₀ which serves as a guide for the layout of the hydraulic profiles.

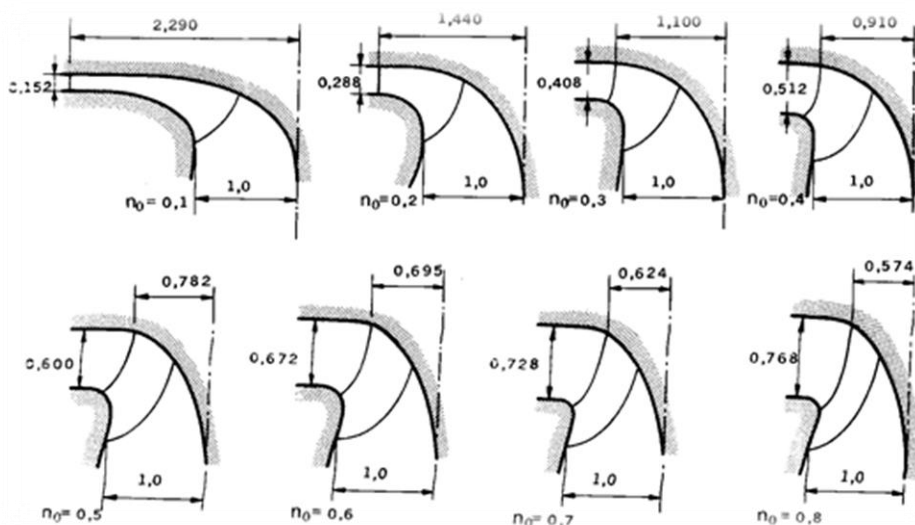


Fig. 1. Variations of the hydraulic profiles.

To draw the hydraulic profile of the turbine composed of curves *i* and *e*, the following equations are used. It is important to highlight that each of the calculated measures are referred to the basic dimension ρ_{2e} shown in Figure 3, said measurement is taken as a unit equal to the radius of point $2e$ [2].

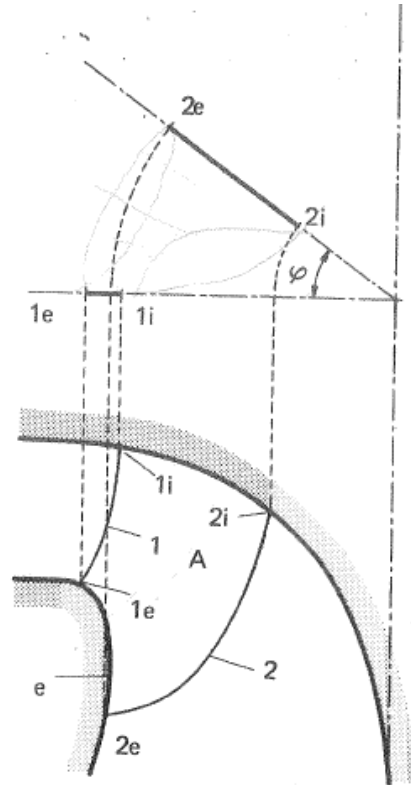


Fig. 2. Limit curves of the volume occupied by the blades.

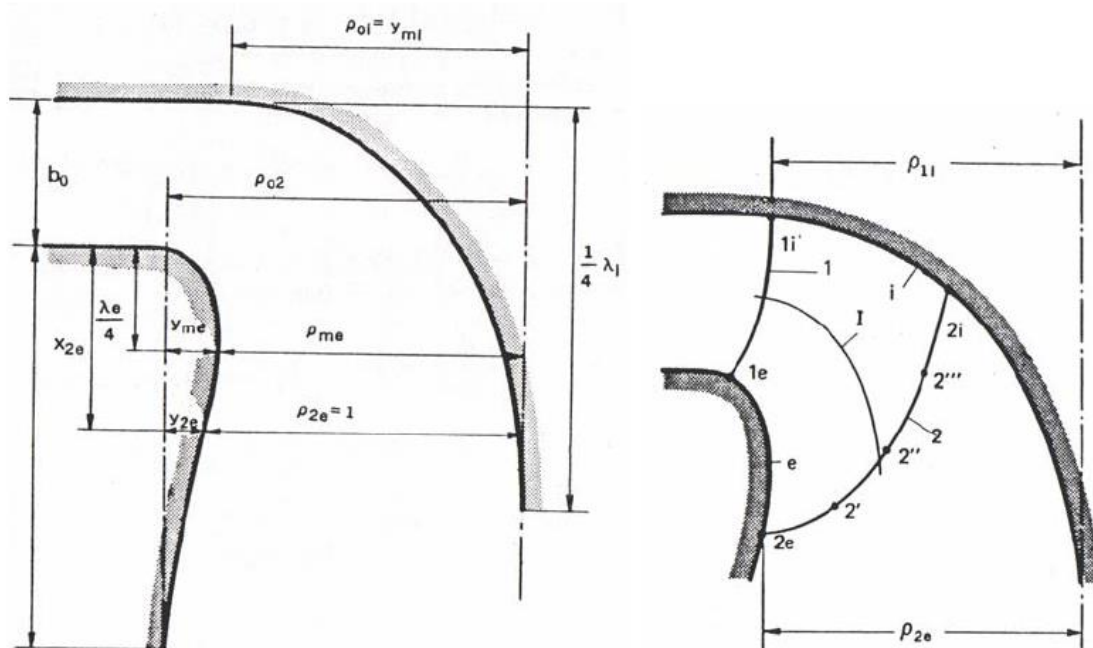


Fig. 3. Typical dimensions of the rotor flow channel

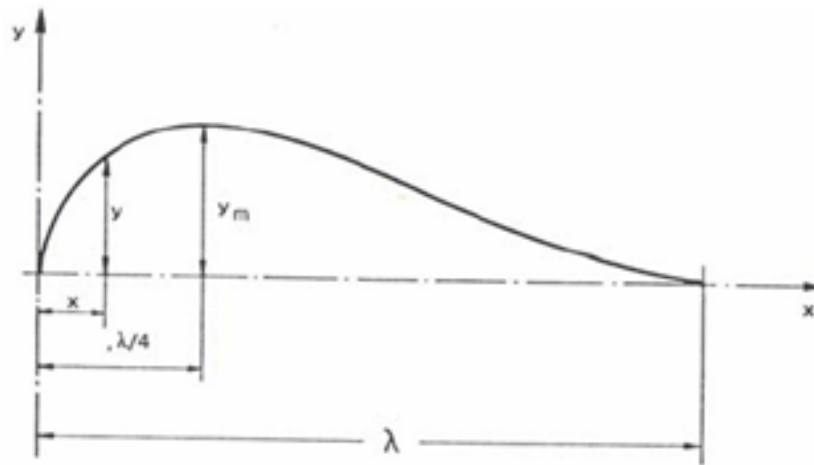


Fig. 4. Boundaries of the curves inside and outside the hydraulic profile

As shown in Figure 4, the internal i and external curves e of the hydraulic profile are defined by the following equation:

$$\frac{y}{y_m} = 3.08 * \left(1 - \frac{x}{\lambda}\right) \sqrt{\frac{x}{\lambda} \left(1 - \frac{x}{\lambda}\right)} \quad (2)$$

Y_m values for the inner curve:

$$y_{mi} = \rho_{oi} = 0.7 + \frac{0.16}{n_o + 0.08} \quad (3)$$

$$\lambda_i = 3.2 + 3.2(2 - n_o)n_o \quad (4)$$

And for the outer curve:

$$\lambda_e = 2.4 + 1.9(2 - n_o)n_o \quad (5)$$

Applying the equation for point $2e$, we have:

$$\frac{y_e}{y_{me}} = 3.08 * \left(1 - \frac{x_{2e}}{\lambda_e}\right) \sqrt{\frac{x_{2e}}{\lambda_e} \left(1 - \frac{x_{2e}}{\lambda_e}\right)} \quad (6)$$

Where it is necessary to determine x_{2e} and y_{2e} .

For x_{2e} , a constant value is taken that is independent of n_o :

$$x_{2e} = 0.5 \quad (7)$$

For y_{2e} :

$$y_{2e} = \rho_{oe} - 1 \quad (8)$$

For ρ_{oe} and other quantities that take into account the geometry of the hydraulic profile, the following values are recommended:

$$\rho_{oe} = \frac{0.493}{n_o^{2/3}} \quad (Forn_0 < 0.275) \quad (9)$$

$$\rho_{oe} = 1.255 - 0.3n_0 \quad (Forn_0 > 0.275) \quad (10)$$

$$b_0 = 0.8(2 - n_0)n_0 \quad (11)$$

Using equation 9 or 10, ρ_{oe} is calculated, this value is taken into equation, and y_{2e} is calculated, and using equation 8, we obtain the relation y_{2e}/y_{me} :

$$y_{me} = \frac{y_{2e}}{y_{2e}/y_{me}} \quad (12)$$

$$\rho_{me} = \rho_{oe} - Y_{me} \quad (13)$$

Determining the actual impeller size [3]

As mentioned above, all dimensions are relative to ρ_{2e} , this measurement will provide the real size of all measurements of the internal and external curves, and its value is calculated, giving a convenient value for the flow coefficient φ_{2e} expressed by the equation 14.

$$\varphi_{2e} = \frac{Q}{n(\rho_{2e})^2} \cdot \frac{1}{u_{2e}} \quad (14)$$

If you substitute $u_{2e} = 2\pi n \rho_{2e}$, the following equation is obtained

$$\rho_{2e} = \left(\frac{Q}{2\pi^2 n \varphi_{2e}} \right)^{1/3} \quad (15)$$

According to turbines previously built and tested, it is known that the value φ_{2e} , to guarantee optimum performance, it is between 0.26 and 0.28, so the average value is selected $\varphi_{2e} \cong 0,270$.

Similarly, you can determine the true value ρ_{li} , in this case, the pressure coefficient u_{li} is used, which is calculated as follows.

$$\psi_{li} = \frac{H}{(u_{li})^2 / 2g} \quad (16)$$

If u_{li} is replaced again and $\psi_{li} = 1.72$ is provided based on the experience in equation 16, the following equation is obtained for ρ_{li}

$$\rho_{li} \cong \frac{60}{2\pi n} \left(\frac{2gH}{1.72} \right)^{1/2} \quad (17)$$

Designing a radial-axial impeller blade in a potential meridional flow (Bowersfeld — Vosnesensky method) [4]

The method of designing the impeller blade in a potential flow was proposed by Bowersfeld in 1913, and then developed by I. N. Vosnesensky. This method has been widely used in engineering practice for designing impellers of radial-axial hydraulic turbines, since it allows reasonably and fairly simply to determine the spatial surface of the impeller blade for given conditions.

The method proposes that the flow in the meridional section of the rotor is potential; therefore, before calculating the blade, it is essential to construct the potential flow and determine the field of constituent meridional speeds in the rotor flow tract obtained by the Bovet method.

In addition, you need to determine the law of change for the product of the variation of the tangential velocity by the radius c_{τ} along some of the border flow lines. It is recommended to give the

dependency $c_u r$ (s) in the form of a straight line or concave curve. It is necessary to assume a theoretical value of hydraulic efficiency.

The main equation that allows by means of numerical integration to find the shape of the blade is

$$\Delta\theta = \frac{r^2\omega - c_u r}{r^2 c_m} \Delta S \quad (18)$$

Using this equation, the angle $\Delta\theta$ in the plane corresponding to the given parameters and to the randomly selected segments ΔS in the current line in the meridional plane of the blade is determined. The sum of the drag angle in the plane $\Theta = \sum \Delta\theta$ must be within the limits accepted for rotors of similar specific speeds. The procedure is graphical analytical and it's described as follows in order to complete the next table.

Table 2. Tabulated results for drag angle calculation

Point	r (m)	$c_u r$ (m ² /s)	r^2	$r^2\omega$	Cm (m/s)	$r^2 c_m$	$\frac{r^2\omega - c_u r}{r^2 c_m}$	(8) _{prom}	Δs (m)	$\Delta\theta$ (rad)	Θ (rad)
1	2	3	4	5	6	7	8	9	10	11	12

- Draw the meridional section of the impeller hydraulic tract on a sufficiently large scale. Plot construction flow lines of the potential flow (not less than 5 lines). Draw the entrance contour of the blade (In Figure 5 $A_1 A_6$) and identify the intersection point of the exit contour with the impeller band. The recommendations for placement of the input contour and point B1 can be determined by analogy with other impellers of the same specific speed. Then line $A_1 B_1$ is divided into equal sections of length 8–10 mm.

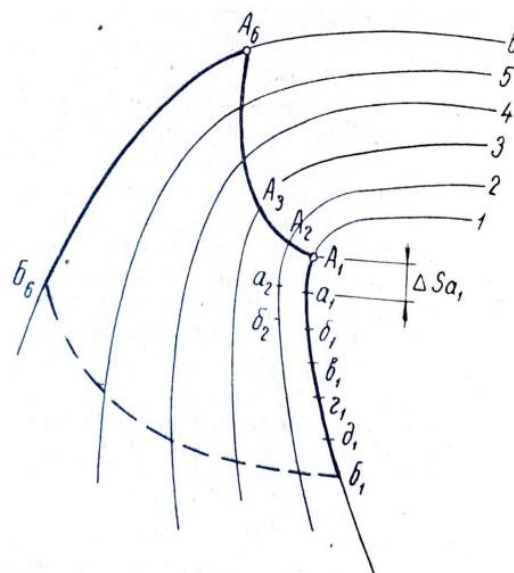


Fig. 5. Hydraulic turbine profile and inlet and outlet contours

- The graph $c_u r$ (s) is constructed for the first current line between limits A_1 and B_1 . For this, the values $c_u r$ for the input contour are determined using the main turbine parameters

$$(C_u r)_{in} - (C_u r)_{out} = \frac{\eta g H}{\omega} \quad (19)$$

It can be assumed that $(c_u r)_{out}=0$, which corresponds to a normal speed at the exit, and therefore

$$(C_u r)_{in} = \frac{\eta g H}{\omega} \quad (20)$$

The input and output contours are in meridional planes and are vortex lines along which $c_u r = \text{const}$. Therefore, the result of the previous equation for the input contour will be the same for all its points and for all the points of the output contour it will be 0.

Having chosen a suitable scale, the $c_u r (s)$ curve is arbitrarily determined, as shown in Figure 5. On the S axis the initial coordinate (point 0) corresponds to point A_1 on the input contour. The section Δs of the flow channel drawing is transferred to the graph and consequently for each of them is found the $c_u r$ value.



Fig. 6. Variants of dependencies $c_{ur} = f(s)$

- The $c_m(s)$ graph representing the change in the meridional velocity along the current line, obtained from the construction of the potential flow, is constructed. From the starting point of the coordinates on the s axis for each current line, the point on the input contour is overlaid (A_1, A_2, \dots, A_6)

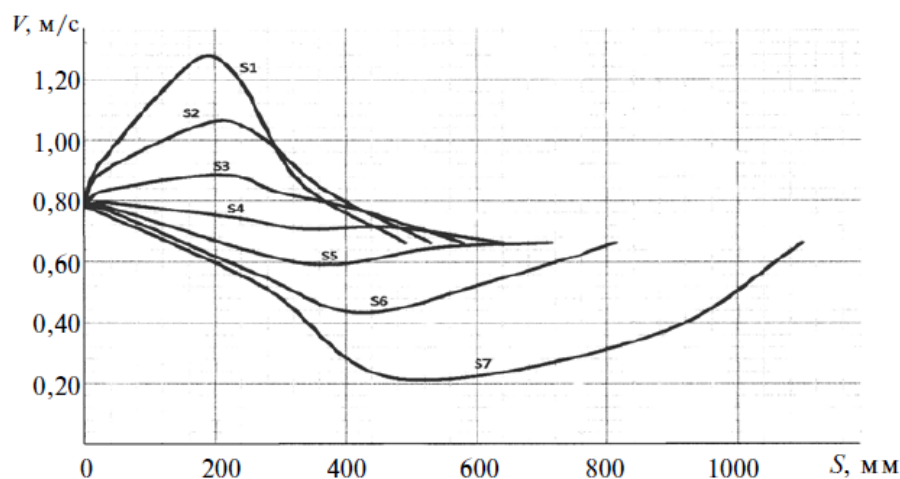


Fig. 7. Variation of meridional velocities along streamlines

- The table previously seen for the first current line is completed. In space 2, the radius values are transferred at points $A_1, a_1, b_1 \dots B_1$, making a direct measurement of the plane of the hydraulic tract. In space 3 the c_{ur} values corresponding to these points of the $c_{ur}(s)$ graph are placed. The spaces

4,5,7,8 are completed by means of calculations. In space 6, by the data of the graph $cm(s)$. In space 9, an average is made between the data in space 8 before and after between lines. In space 10 there are the values Δs between points $A_1, a_1, b_1 \dots B_1$ at real scale. The values to be placed in space 11 result from multiplication $(9) \times (10)$. In spaces 12 and 13, the values Θ of the angles in radians and degrees in summation are transferred, measuring from the input contour (from point A_1) using equation 18.

- Line A_1B_1 is constructed in the plane. The horizontal line OA_1 corresponds to the meridional section in which the entrance contour is located. The meridional surface on which point a_1 is rotated with respect to point OA_1 at an angle $\Delta\Theta_a$, which is taken from the table. With the radius r_a , the point is cut on the line $0a_1$ and the points A_1 and a_1 are joined. Subsequently, the angles $\Delta\Theta_{b_1}, \Delta\Theta_{B_1}$ are placed and the points corresponding to the radius are cut in the lines, the polyline which represents the current line $A_1 B_1$ in the plane is found. The central angle between the lines OA_1 and OB_1 is the drag angle of the blade.

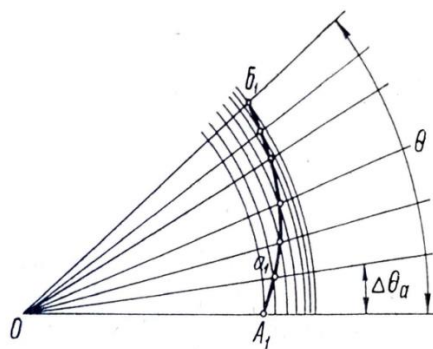


Fig. 8. Planar and meridional coordinates of the surface of the turbine blade

- The calculation is completed for the following current lines. The task is to find sections $\Delta S_{A_2}, \Delta\Theta_{a_2}$ that, after carrying out the calculation of the table, must obtain the same angles $\Delta\Theta_a, \Delta\Theta_b, \Delta\Theta_B$ as those previously obtained in the first line and are contained within the drag angle.

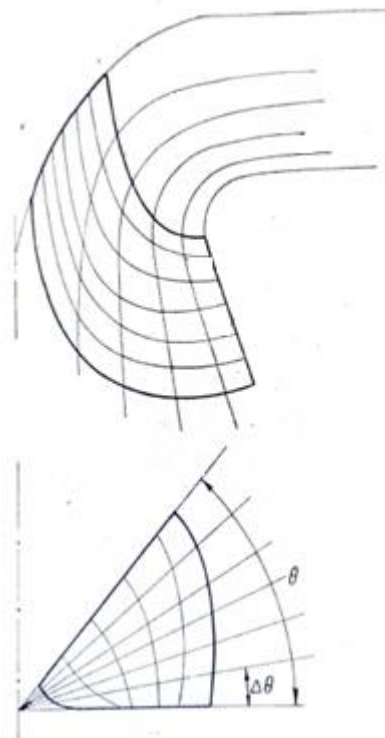


Fig. 9. Planar and meridional coordinates of the surface of the turbine blade

Mathematical model. In order to obtain the hydrodynamic modeling, the following equations were used:

Equation of continuity of the liquid medium:

$$\frac{\partial \bar{u}_x}{\partial x} + \frac{\partial \bar{u}_y}{\partial y} + \frac{\partial \bar{u}_z}{\partial z} = 0, \quad (21)$$

Where \bar{u}_i — time-averaged projections of fluid velocities on the corresponding axes;

Equation of the change in the amount of motion averaged over time:

$$\rho \left[\frac{\partial \bar{u}_i}{\partial t} + \bar{u}_j \frac{\partial \bar{u}_i}{\partial x_j} \right] = - \frac{\partial \bar{p}}{\partial x_i} + \frac{\partial}{\partial x_i} \left[T_{ij}^{(v)} - \rho u_i u_j \right], \quad (22)$$

Where $\bar{u}_i \bar{p}$ — averaged speed and pressure;

$\tilde{T}_{ij}^{(v)} = 2\mu \tilde{s}_{ij}$ — viscous stress tensor for incompressible fluid;

$\tilde{s}_{ij} = \frac{1}{2} \left[\frac{\partial \bar{u}_i}{\partial x_j} + \frac{\partial \bar{u}_j}{\partial x_i} \right]$ — strain rate tensor;

$\rho u_i u_j$ — Reynolds stresses.

The Reynolds system of equations is open due to the presence of unknown Reynolds stresses. The system is closed using the k- ω SST turbulence model.

Terms of computer simulation. In the process of the computer simulation, a three-dimensional model of the flow part of the turbine was created, and physical models and parameters of the computational grid were set for it. The density value remained unchanged throughout the experiment. For the boundary conditions, the inlet and outlet pressure values were determined to create a pressure drop equal to the nominal pressure (see Table 3). The rotation speed is preliminarily assigned based on the initial turbine design conditions. Impeller torque and flow rates measured due to pressure drop were measured.

Table 3. Initial conditions

Parameter	Value
Input stagnation	711125,0 Pa
Outlet pressure	0,0 Pa
Rotational speed	300 rpm

To build the grid, the following construction models were selected:

- Generator of polyhedral cells;
- surface mesh generator;
- Prismatic layer generator.

The grid parameters are shown in Table 4:

Table 4. The parameters of the computational grid

Parameter	Value
Base size	50 mm
Prismatic Stretching	1.3
Prismatic layer thickness, relative to the base size	50%
The number of prismatic layers	5
Number of Cells Generated on Impeller	7541332
The number of generated cells on Inlet	5096089
The number of generated cells on Outlet	1024312

In the impeller, the mesh was thinned 2 times to reduce the calculation error. The resulting mesh in the cross section of the flow part is shown in Fig. 4:

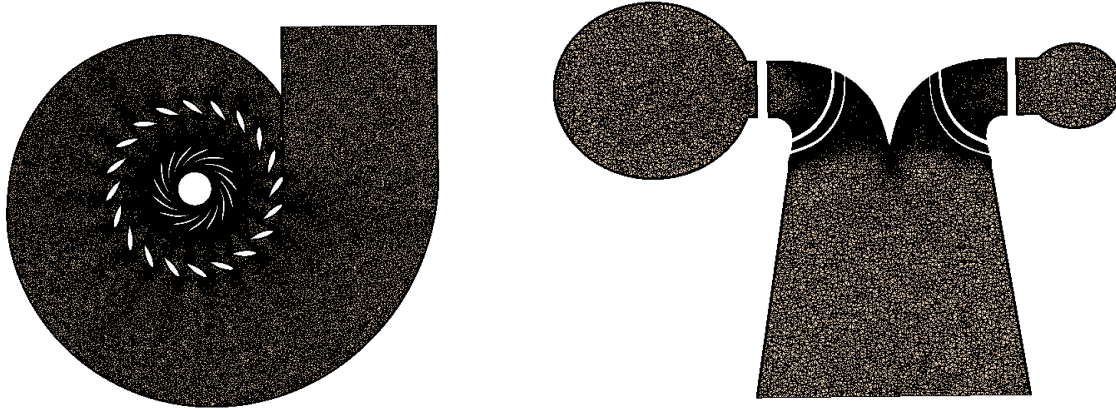


Fig. 10. The resulting mesh in the cross section of the flowing part

Results

Applying the Bovet method the geometry of the hydraulic tract is obtained using the main design parameters of the turbine $Q = 50 \text{ m}^3/\text{h}$; $H = 72.5 \text{ m}$; $P = 33 \text{ MW}$ and applying the Bowersfeld — Vosnesenskymethod, the geometry of the blade is obtained.

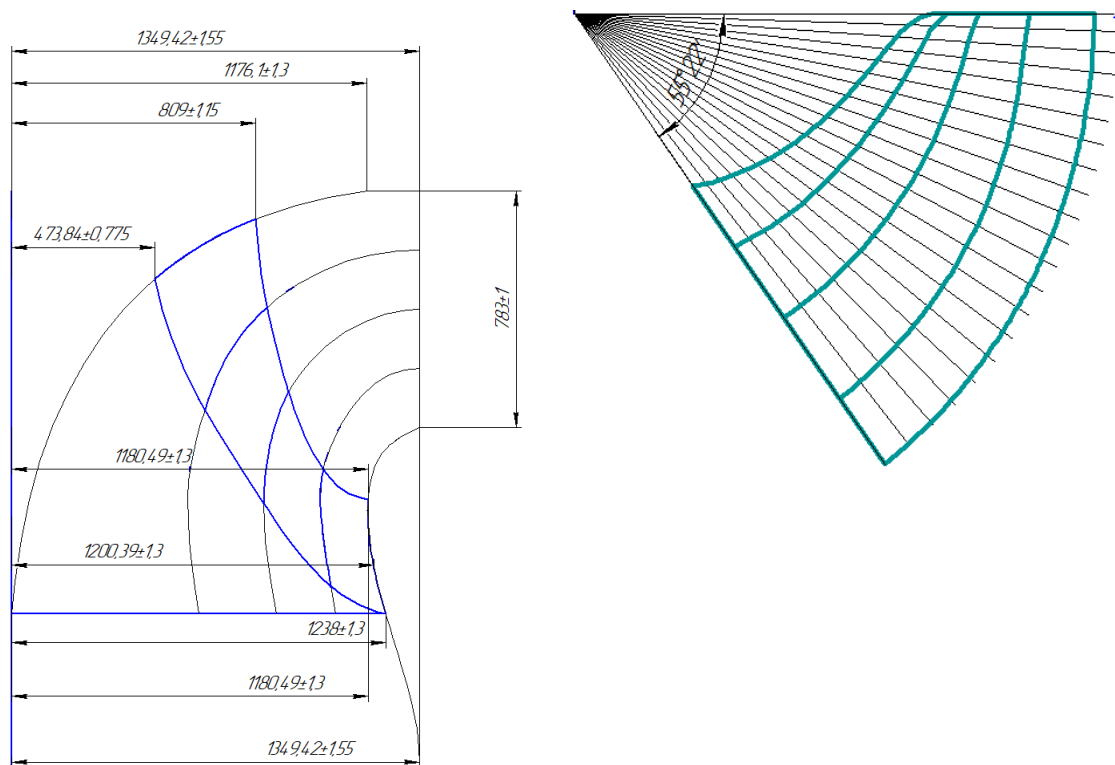


Fig. 11. Dimensions and Coordinates obtained

The spiral chamber, the distributor and the discharge tube take their dimensions based on the nominal diameter of the impeller. The geometry of the simulated turbine is constructed using CAD programs [5]. The CFD program is used to obtain various parameters of the turbine, changing the angle on the distributor. The results calculated are shown in Table 5.

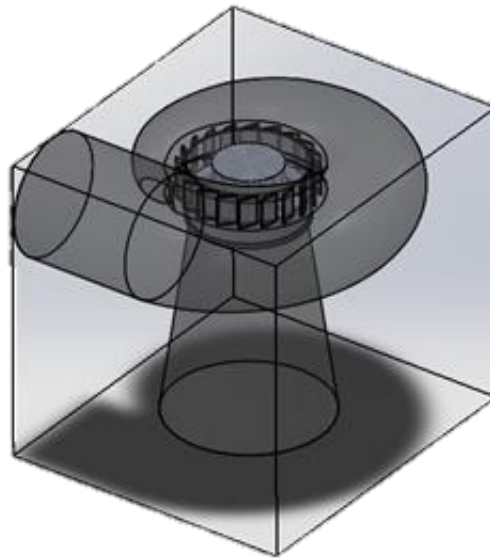


Fig. 12.Hydraulic model of the turbine composition

Table 5. Parameters obtained

Distributor opening (grades)	Flow Rate (m^3 / s)	Head (m)	Torque (Nm)	Power impeller (MW)	Power fluid (MW)	Efficiency
26	28.93	71.75	378062.63	11.88	20.36	58.80%
30	43.6	69.66	627163.53	19.70	29.79	64.00%
33	46.3	69.89	693619.86	21.79	31.74	68.00%
35	48.55	69.66	723487.34	22.73	33.18	68.40%
38	51.83	69.26	747819.34	23.49	35.22	66.00%
40	53.77	69	758076.03	23.82	36.40	65.00%
43	57.48	68.4	762232.88	23.95	38.57	62.00%
46	60.36	67.85	744574.59	23.39	40.18	58.00%

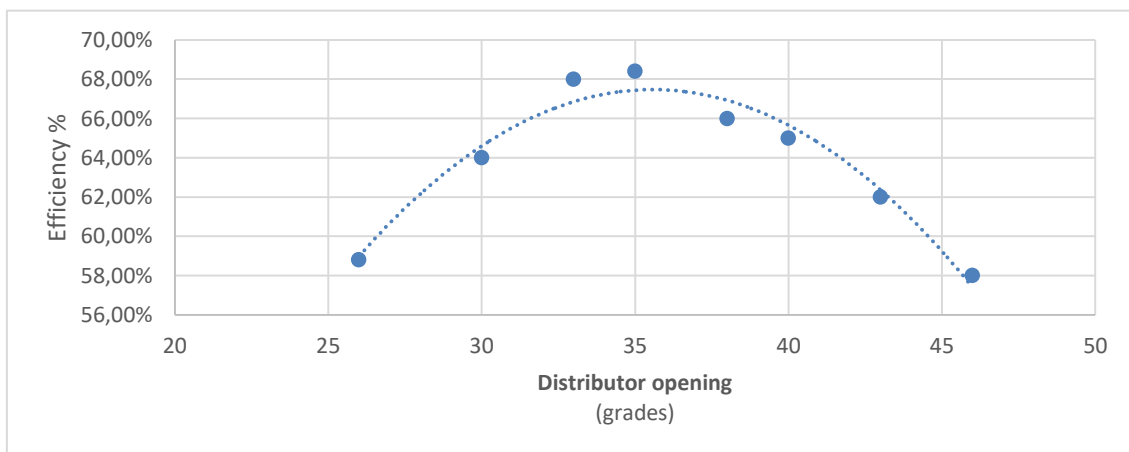


Fig. 13. Efficency graph

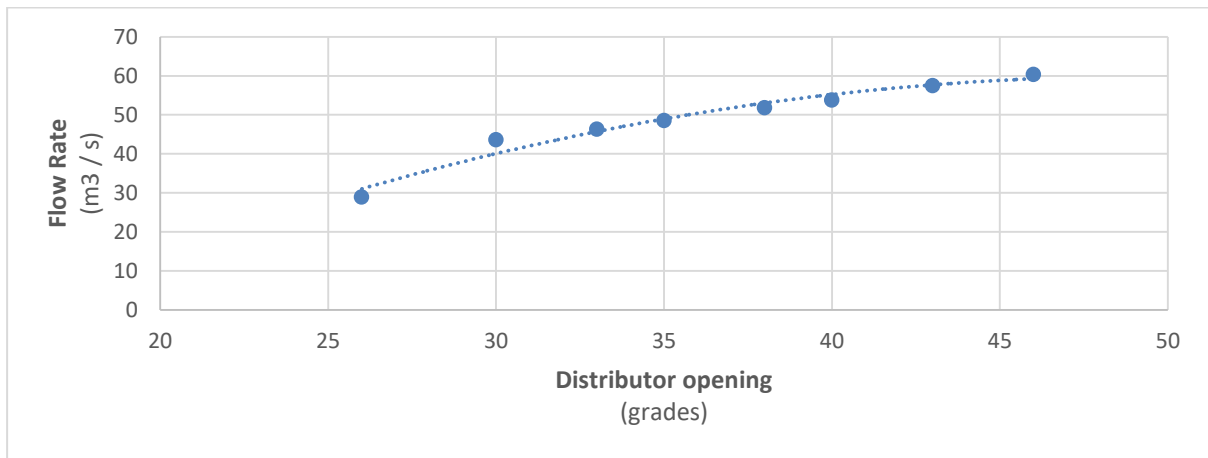


Fig. 14. Flow Rate graph

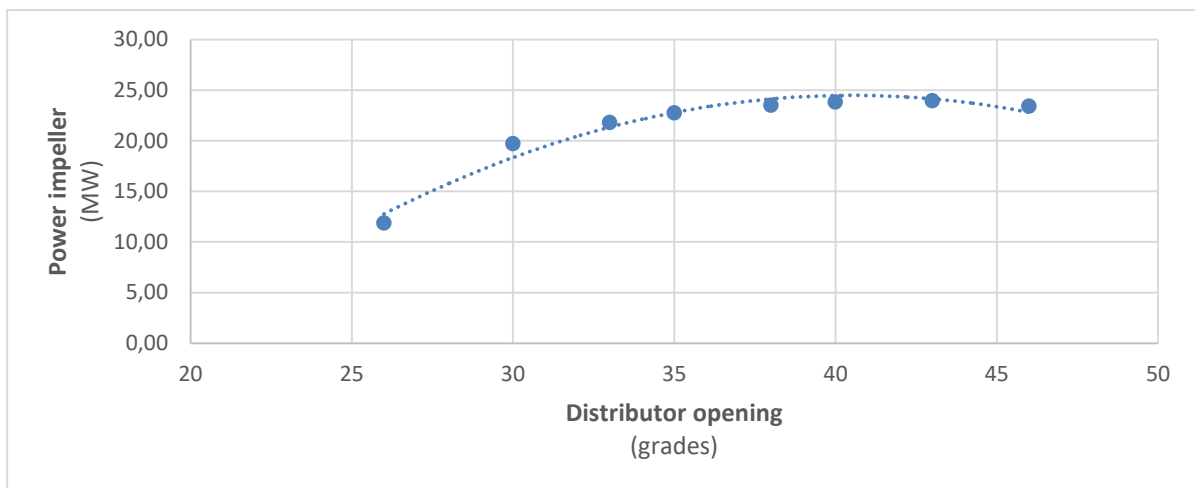


Fig. 15. Power on the Impeller Graph

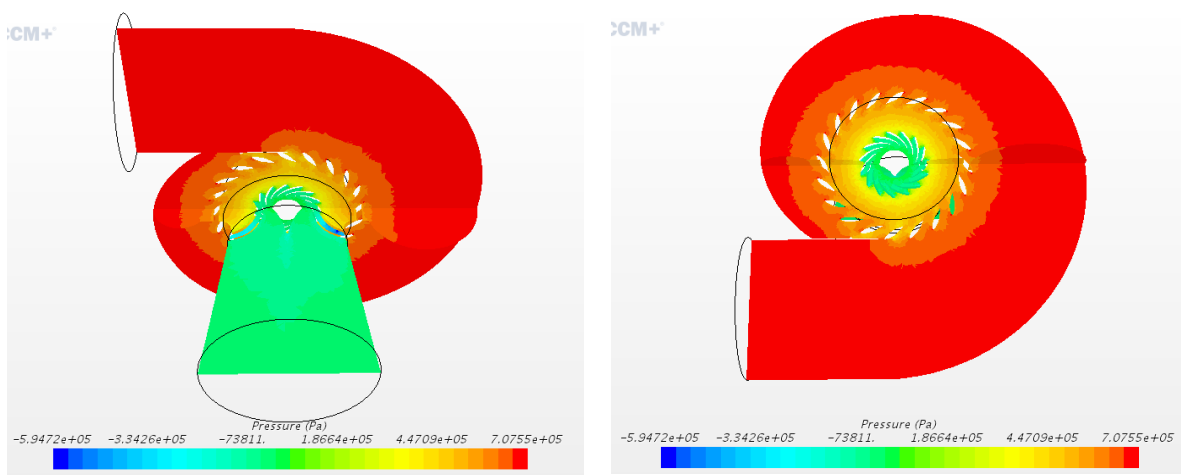


Fig. 16. Pressure distribution in the hydraulic circuit

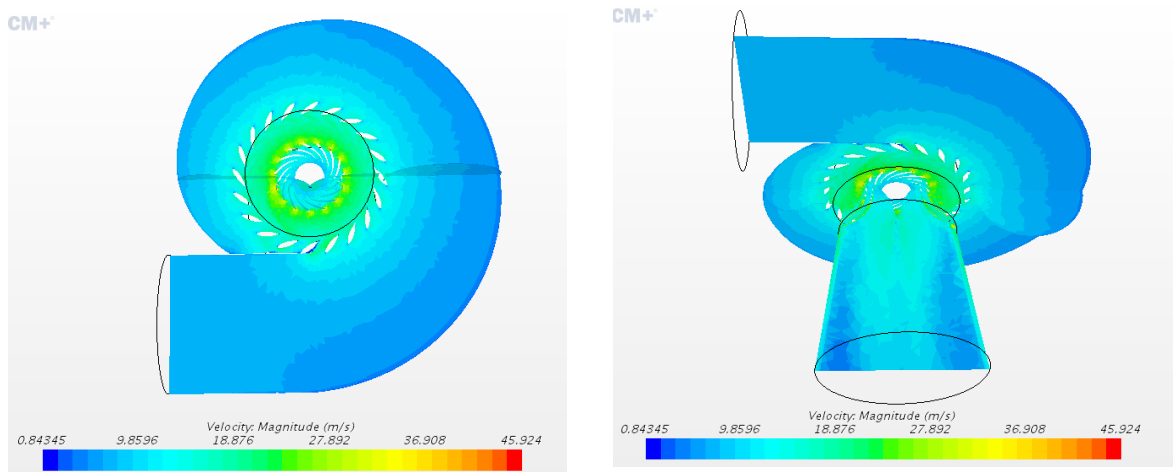


Fig. 17. Speed distribution in the hydraulic path

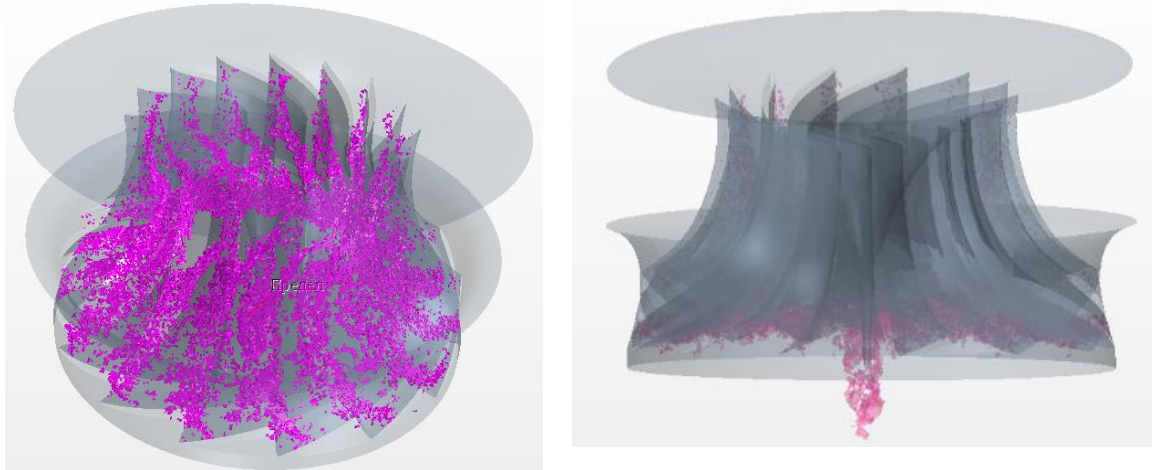


Fig. 18. The presence of cavitation in the impeller

Conclusion

As a result of the experiment, it can be concluded that a Radial Axial Turbine was designed with the following specifications: Net height of 72.5 m, installation flow 50 m³ / s. For this point of operation, an overall efficiency of 93% is projected. The behavior of the parameters is that expected for an axial radial type turbine, in which when the distributor is opened, the flow is increased, having a constant head, reaching an efficiency of 68.4% at an opening of 35 degrees and a flow rate of 48.55 m³ / s

The traditional design for Radial Axial Turbine impellers design, specifically the Bover and Bowersfeld — Vosnesensky Methods, can be applied in the design of a functional, achieving an acceptable performance according to the efficiency results obtained from the 3D numerical simulations. Nevertheless, considering that the process is iterative, the results cannot be expected to be optimal at the first attempt, so it is necessary to repeat the process until the best results are achieved. In conclusion, we must add that the obtained efficiency has a lower value than that of analogues, since this model has not yet been optimized in CFD packages. However, the power value is acceptable, which means that further modeling should lead to an increase in efficiency based on optimization methods of the flow part.

Literature

- [1] Bover, T. Contribution of the study of trace of blading of a reaction turbine of the Francis type (1963) New York ASME Winter Meeting 1961, pp. 47–79.

- [2] Mataix, C. “Hydraulic Hydromachines” (2003) Editorial ICAI
- [3] Vasiliev Yu. S. Samorukov I. S. Khlebnikov. S. N. Basic energy equipment of hydro power plants. Composition and selection of basic parameters (2002) Saint Petersburg State Polytechnical University
- [4] Topazh, G. I. The Basics of the Working Process and Calculation of Hydro Turbines (2011) Saint Petersburg State Polytechnical University, pp. 139–151
- [5] De Andrade Correia, J. A. Mechanical and Hydraulic Design for a Tubular Francis Turbine (2006) Simon Bolivar University
- [6] Busyrev, A.I. Topazh, G.I. Selection of basic parameters and elements of the flowing part of reactive hydroturbines (2006) Saint Petersburg State Polytechnical University
- [7] Laubah D.V. Design of the flow part and the rotation mechanism of the vanes of the guide vane for the Myatlinskaya HPP (2017) Saint Petersburg State Polytechnical University
- [8] Barlit V.V. Hydraulic turbines (1977) Editorial Union “Vishcha Shkola”, pp. 360
- [9] Kovalev, N. N. “Hydroturbines” (1971), Editorial “Mashinostroenie”, Leningrad.
- [10] Morales, M. P. Francis Turbines Design in C++ Builder (2000) Costa Rica University, pp. 125–136
- [11] Mathematical modeling of the mechanisms of volumetric hydraulic machines. S. Semenov and D. Kulakov 2019 IOP Conf. Ser.: Mater. Sci. Eng. 492 012042
- [12] The effect of design parameters of the closed type regenerative pump the energy characteristics. N Isaev 2019 IOP Conf. Ser.: Mater. Sci. Eng. 492 012026
- [13] Hydrodynamic modelling of the impact of viscosity on the characteristics of a centrifugal pump. V Tkachuk 2019 IOP Conf. Ser.: Mater. Sci. Eng. 589 012007
- [14] The development of the theory of calculation of the hydrodynamic coupling. V Lomakin 2019 IOP Conf. Ser.: Mater. Sci. Eng. 492 012012
- [15] N Egorkina and A Petrov 2019 IOP Conf. Ser.: Mater. Sci. Eng. 492 012015
- [16] A Petrov 2019 IOP Conf. Ser.: Mater. Sci. Eng. 492 012036